

Effect of excitation loads on the low frequency structural responses of a submerged hull

Cong Zhang (1) and Nicole Kessissoglou (1)

(1) School of Mechanical and Manufacturing Engineering, The University of New South Wales, Sydney, Australia

ABSTRACT

This paper studies the effect of different excitation loads on the low frequency vibrational behaviour of a submerged hull. The submerged hull is modelled as a fluid-loaded cylindrical shell closed at each end by circular plates. The external pressure acting on the hull due to the fluid loading is analytically calculated using an infinite model. To simulate excitation of the hull from propeller fluctuating forces, both axial and radial excitation was simultaneously considered. The effect of varying the degrees of load in the axial and radial directions on the hull structural responses, in particular, on the hull breathing and bending modes, is examined.

INTRODUCTION

Many engineering structures have the basic form of thin-walled cylindrical shells; for example, aircraft fuselages, pipes and ducts, submarine pressure hulls and fluid storage tanks. The analysis of vibration characteristics of thin-walled circular cylindrical shells is important in cases where the ratio of cylinder radius to wall thickness is large, as in aircraft fuselages and submarine pressure hulls. The dynamic responses of thin cylindrical shells have received much research attention, ranging from the free vibrational characteristics of cylindrical shells with different boundary conditions (Leissa 1993, Yu 1955, Forsberg 1964), stiffened cylindrical shells (Mukhopadhyay and Sinha 1992), coupled cylinder/plate structures (Tso and Hansen 1995), and cylindrical shells with various end closures (Galletly and Mistry 1974). A review on the vibrations of cylindrical shells with and without fluid structure interaction is given by Amabili and Paidoussis (2003).

The fundamental component of a submarine is the pressure hull. A submarine propeller can excite low frequency global hull modes due to unsteady forces generated on the blades which are transmitted via the shafting system. The propeller fluctuating forces at the propeller hub occur in axial, tangential and radial directions. The radial and axial components can be of similar magnitude (Breslin and Andersen 1994), resulting in global hull axial resonances which are predominantly excited by the axial forces, and hull bending modes which are excited by the radial forces transmitted directly to the hull via the aft end journal bearing.

This work examines the low frequency dynamic responses of a submerged hull. The pressure hull is essentially a cylindrical steel shell modelled using thin shell theory. The hull is idealised as a fluid-loaded cylindrical shell closed at each end by circular plates. Both axial and radial excitation on the aft end of the hull is considered. The effect of the different excitation cases on the hull structural responses, in particular, on the shell breathing and bending motion, is examined.

DYNAMIC MODEL OF THE SUBMERGED HULL

Cylindrical shell

For a cylindrical shell, the axial u_c , circumferential v_c and radial w_c motions are the orthogonal components of the cylinder displacement in the x , θ and z directions, respectively. As shown in Fig. 1, a is the mean radius of the shell, h_c is the thickness and L is the length of the cylinder. As the density of the water is similar to the density of steel, the fluid-loading effect has to be considered in the dynamic modelling of a submarine hull.

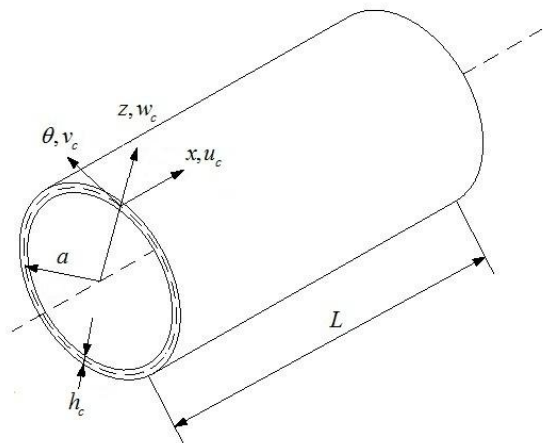


Figure 1. Coordinate system and displacements for a thin cylindrical shell

The uniform cylinder is modelled using Flügge equations of motion which are given by (Leissa 1993)

$$\frac{\partial^2 u_c}{\partial x^2} + \frac{(1-\mu_c)}{2a^2}(1+\beta^2)\frac{\partial^2 u_c}{\partial \theta^2} + \frac{1+\mu_c}{2a}\frac{\partial^2 v_c}{\partial x \partial \theta} + \frac{\mu_c}{a}\frac{\partial w_c}{\partial x} - \beta^2 a \frac{\partial^3 w_c}{\partial x^3} + \beta^2 \frac{(1-\mu_c)}{2a}\frac{\partial^3 w_c}{\partial x \partial \theta^2} - \frac{1}{c_{lc}^2}\frac{\partial^2 u_c}{\partial t^2} = 0 \quad (1)$$

$$\frac{1+\mu_c}{2a} \frac{\partial^2 u_c}{\partial x \partial \theta} + \frac{(1-\mu_c)}{2} \frac{\partial^2 v_c}{\partial x^2} + \frac{1}{a^2} \frac{\partial^2 v_c}{\partial \theta^2} + \frac{1}{a^2} \frac{\partial w_c}{\partial \theta} + \beta^2 \left(\frac{3(1-\mu_c)}{2} \frac{\partial^2 v_c}{\partial x^2} - \frac{(3-\mu_c)}{2} \frac{\partial^3 v_c}{\partial x^2 \partial \theta} \right) - \frac{1}{c_{Lc}^2} \frac{\partial^2 v_c}{\partial t^2} = 0 \quad (2)$$

$$\beta^2 \left(a^2 \frac{\partial^4 w_c}{\partial x^4} + 2 \frac{\partial^4 w_c}{\partial x^2 \partial \theta^2} + \frac{1}{a^2} \frac{\partial^4 w_c}{\partial \theta^4} - a \frac{\partial^3 u_c}{\partial x^3} + \frac{(1-\mu_c)}{2a} \frac{\partial^3 u_c}{\partial x \partial \theta^2} - \frac{(3-\mu_c)}{2} \frac{\partial^3 v_c}{\partial x^2 \partial \theta} + \frac{2}{a^2} \frac{\partial^2 w_c}{\partial \theta^2} \right) + \frac{\mu_c}{a} \frac{\partial u_c}{\partial x} + \frac{1}{a^2} \left(\frac{\partial v_c}{\partial \theta} + w_c(1+\beta^2) \right) + \frac{1}{c_{Lc}^2} \frac{\partial^2 w_c}{\partial t^2} - \frac{p_a}{c_{Lc}^2 \rho_c h_c} = 0 \quad (3)$$

where E_c , ρ_c and μ_c are respectively Young's modulus, density and Poisson's ratio of the hull. $c_{Lc} = \sqrt{E_c / \rho_c (1 - \mu_c^2)}$ is the longitudinal wave speed. $\beta = h_c / \sqrt{12}a$ is a non-dimensional thickness parameter. For a fluid-loaded cylinder, the external pressure p_a in equation (3) is given by (Junger and Feit 1986)

$$p_a = \frac{\rho_c h_c c_{Lc}^2}{a^2} F_L w_c \quad (4)$$

$$F_L = \begin{cases} -\Omega^2 \frac{a}{h_c} \frac{\rho_f}{\rho_c} \frac{H_n(\beta_f)}{\beta_f H'_n(\beta_f)} & k_f > k_n \\ -\Omega^2 \frac{a}{h_c} \frac{\rho_f}{\rho_c} \frac{K_n(\beta_f)}{\beta_f K'_n(\beta_f)} & k_f < k_n \end{cases} \quad (5)$$

$$\beta_f = \begin{cases} a \sqrt{k_f^2 - k_n^2} & k_f > k_n \\ a \sqrt{k_n^2 - k_f^2} & k_f < k_n \end{cases} \quad (6)$$

where $\Omega = \omega a / c_{Lc}$ is the non-dimensional ring frequency, $k_f = \omega / c_f$ is the fluid wavenumber, and ρ_f , c_f are respectively the density and speed of sound in the fluid. k_n is the hull axial wavenumber and ω is the radian frequency. H_n is the Hankel function of order n . K_n is the modified Bessel function of order n . H'_n and K'_n are their derivatives with respect to the argument.

General solutions for the cylindrical shell displacements can be written as

$$u_c(x, \theta, t) = U e^{jk_n x} \cos(n\theta) e^{-j\omega t} \quad (7)$$

$$v_c(x, \theta, t) = V e^{jk_n x} \sin(n\theta) e^{-j\omega t} \quad (8)$$

$$w_c(x, \theta, t) = W e^{jk_n x} \cos(n\theta) e^{-j\omega t} \quad (9)$$

where U , V , W are the amplitudes of the axial, circumferential and radial displacements, respectively, which are determined from the boundary conditions. These solutions represent a wave travelling in the axial direction and standing with n nodal lines in the circumferential direction. Substituting the general solutions given by equations (7)-(9) into the equations of motion results in three linear equations in terms of U , V and W . These linear equations can be arranged in

matrix form as $\mathbf{A}\mathbf{X} = \mathbf{0}$, where $\mathbf{X} = [U \quad V \quad W]^T$. For a non-trivial solution, the determinant of matrix \mathbf{A} must be zero. The expanded determinant results in a characteristic equation in terms of k_n and ω . For each ω , the determinant is a polynomial of eighth order in terms of k_n . Due to the Hankel and Bessel functions in equation (5), the characteristic equation is non-linear and must be solved using a numerical solution as described by Scott (1988) and Caresta et al. (2010).

Circular plate

The pressure hull is closed at each end by circular plates. The equations of motion for bending w_p and in-plane u_p , v_p motions of a circular plate can be found in Leissa (1993). General solutions for plate displacements are given by (Tso and Hansen 1995)

$$w_p = \sum_{n=0}^{\infty} \left(A_{n,1} J_n(k_{pB} r) + A_{n,2} I_n(k_{pB} r) \right) \cos(n\theta) e^{-j\omega t} \quad (10)$$

$$u_p = \sum_{n=0}^{\infty} \left(B_{n,1} \frac{\partial J_n(k_{pL} r)}{\partial r} + \frac{n B_{n,2} J_n(k_{pL} r)}{r} \right) \cos(n\theta) e^{-j\omega t} \quad (11)$$

$$v_p = -\sum_{n=0}^{\infty} \left(\frac{n B_{n,1} J_n(k_{pL} r)}{r} + B_{n,2} \frac{\partial J_n(k_{pL} r)}{\partial r} \right) \sin(n\theta) e^{-j\omega t} \quad (12)$$

where r is the radial coordinate from the centre of the circular plate. $k_{pB} = (\rho_p \omega^2 h_p / D_p)^{1/4}$ is the plate bending wavenumber. $k_{pL} = \omega \sqrt{\rho_p (1 - \mu_p^2) / E_p}$, $k_{pT} = \omega \sqrt{2\rho_p (1 + \mu_p) / E_p}$ are the wavenumbers for in-plane waves in the plate. E_p , ρ_p and μ_p are the Young's modulus, density and Poisson's ratio of the circular plate. h_p is the plate thickness. J_n and I_n are respectively the Bessel function and modified Bessel function of the first kind of order n . The coefficients $A_{n,i}$ and $B_{n,i}$ ($i=1,2$) are determined from the boundary conditions.

Boundary equations

The displacements and slopes of the cylindrical shell and circular end plate at the coupling junction are shown in Fig. 2. Similarly, the forces and moments of the shell and plate at the coupling junction are shown in Fig. 3.

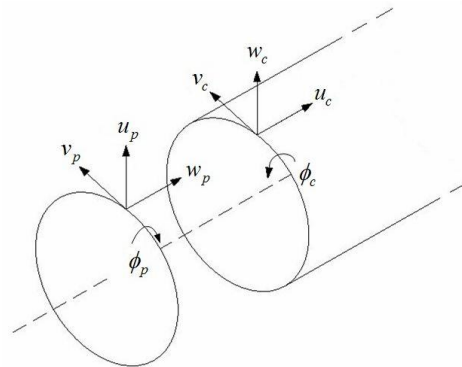


Figure 2. Displacements and slopes of the cylindrical shell and circular end plate

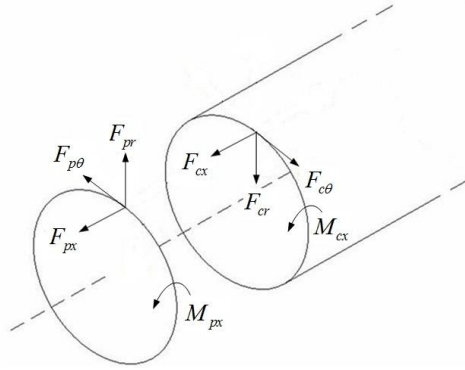


Figure 3. Forces and moments of the cylindrical shell and circular end plate

At the free ends of the cylindrical shell corresponding to $x=0$ and L , the continuity equations of the displacements and slope between the shell and end plates are as follows

$$u_p = w_c, \quad w_p = u_c \quad (13,14)$$

$$v_p = v_c, \quad \frac{\partial w_p}{\partial r} = -\frac{\partial w_c}{\partial x} \quad (15,16)$$

Equilibrium of the forces and moments are given by

$$F_{cx} + F_{px} = 0, \quad F_{c\theta} - F_{p\theta} = 0 \quad (17,18)$$

$$M_{cx} + M_{px} = 0, \quad F_{cr} - F_{pr} = 0 \quad (19,20)$$

F_{cx} , F_{cr} , $F_{c\theta}$, M_{cx} are the internal force and moment expressions for the cylindrical shell. F_{px} , F_{pr} , $F_{p\theta}$, M_{px} are the internal force and moment expressions for the circular plates. The various force and moment equations can be found in Leissa (1993).

Excitation load cases

Two excitation cases were considered corresponding to axial and radial excitation. These forces were applied separately and then simultaneously. Axisymmetric excitation was generated by applying an axial force to the centre of the circular plate. Asymmetric excitation was generated using a radial point force at the end of the end plate. When these two excitation cases were simultaneously considered, a weighting was applied to each force. The weightings were varied to examine the effect of different axial and radial load combinations on the hull structural responses. Five axial and radial excitation cases listed in Table 1 are examined in this work.

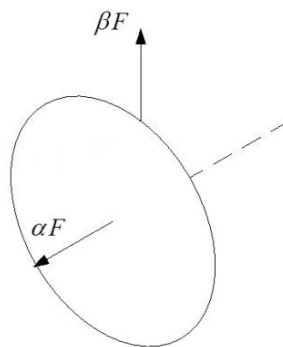


Figure 4. Axial and radial excitation load cases

Table 1. Various axial and radial excitation cases

| | Axial excitation weighting α | Radial excitation weighting β |
|--------|-------------------------------------|-------------------------------------|
| Case 1 | 1 | 0 |
| Case 2 | 0.75 | 0.25 |
| Case 3 | 0.5 | 0.5 |
| Case 4 | 0.25 | 0.75 |
| Case 5 | 0 | 1 |

The axial force applied to the centre of the end plate was dynamically modelled by separating the circular plate into an inner circular plate of very small radius and an outer annular plate (Caresta 2011). The point force at the centre of the plate was then approximated as a distributed force applied axially at the junction of the annular and inner circular plates.

For the asymmetric excitation case, a radial point force was applied to the edge of the end plate, as shown in Fig. 4. The point force located at $(x_0, \theta_0) = (0,0)$ is described in terms of the Dirac delta function. The external force results in modification to the equilibrium of the force given by equation (20) at $x=0$, which now becomes

$$F_{cr} - F_{pr} = F_0 \delta(x - x_0) \delta(\theta - \theta_0) e^{-j\omega t} \quad (21)$$

Excluding the time harmonic dependency, multiplying the above equation by $\cos(n\theta)$ and then taking the integral from $-\pi$ to π , equation (21) becomes

$$F_{cr}|_{x_0} - F_{pr}|_{x_0} = \varepsilon F_0 \cos(n\theta_0) \quad (22)$$

where $\varepsilon = 1/2\pi a$ if $n=0$ and $\varepsilon = 1/\pi a$ if $n \neq 0$, where n is the circumferential mode number.

The dynamic response of the entire hull is expressed in terms of unknown coefficients, $W_{n,i}$ ($i=1:8$), for the cylindrical shell and unknown coefficients, $A_{n,i}$ and $B_{n,i}$ ($i=1,2$), for the circular end plates. The dynamic response of the hull is calculated by assembling a matrix from the boundary and continuity equations $\mathbf{B}\mathbf{X} = \mathbf{F}$ where \mathbf{X} is the vector of the unknown displacement coefficients and \mathbf{F} is the force vector. Solving the system for each circumferential mode n gives the steady state shell displacements at a certain frequency ω .

RESULTS

The frequency response functions (FRFs) of the shell displacements are presented for a cylindrical shell of radius 3.25m, hull thickness 0.04m, length 45m and with two end plates of thickness 0.04m. The material properties for steel were used for both the shell and plates, with density of 7800kgm^{-3} , Young's modulus of $2.1 \times 10^{11}\text{Nm}^{-2}$ and Poisson's ratio of 0.3. Structural damping was introduced using a complex Young's modulus $E(1 - j\eta)$ where $\eta = 0.02$ is the structural loss factor. The surrounding fluid has density of 1500kgm^{-3} and speed of sound of 1500ms^{-1} .

The FRFs were measured at the outer edge of the circular plate corresponding to the driving point location of the radial force. The amplitudes of the external axial and radial forces are unity ($F_0 = 1$). The FRFs are calculated considering all the circumferential modes in the range $n=0:10$.

The effects of the various excitation cases listed in Table 1 on the axial and radial responses of the cylindrical shell are shown in Figs. 5 to 7. Excitation at the centre of the end plate gives rise to an axisymmetric case in which the zeroth circumferential shell modes are predominantly excited. The submerged hull follows rigid body motion at very low frequencies. The peaks at frequencies of around 9, 35, and 80Hz in Fig. 5 are caused by resonances of the end plates. The peak at 58 Hz in the axial displacement corresponds the first axial mode for the $n=0$ circumferential modes of the cylindrical shell, at which the shell is in breathing motion. Only the resonances of the end plates are observed in the radial response in Fig. 5.

In Fig. 6, it is observed that radial excitation at the edge of the end plate gives rise to an asymmetric case in which the $n=1$ circumferential modes are predominantly excited. For this case, the shell is in bending motion. All the peaks in the axial and radial responses in Fig. 6 correspond to $n=1$ modes of various orders.

Comparison of Figs. 5 and 6 shows that for the asymmetric case due to radial excitation at the edge of the end plate, a significantly greater number of $n=1$ modes are excited compared to the number of $n=0$ modes for the axisymmetric case due to axial excitation at the centre of the end plate. This is attributed to the fact that the modal density of the cylindrical shell for the radial modes is significantly greater than that for the axial modes which occur at widely spaced intervals.

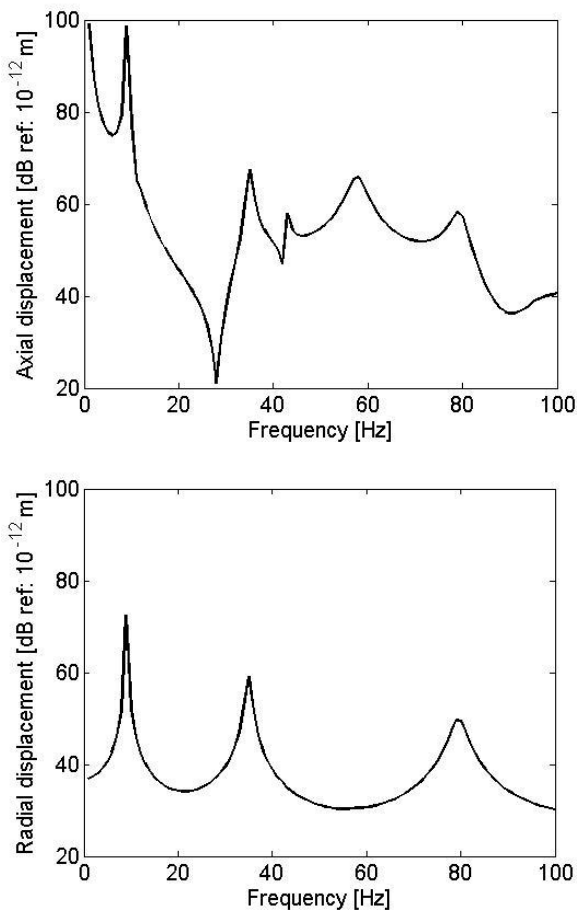


Figure 5. Axial and radial responses due to axial excitation at the centre of the end plate ($\alpha=1$ and $\beta=0$)

The results in Fig. 7 were obtained using simultaneous axial and radial force excitation with different proportions of force as listed by cases 2 to 4 in Table 1. The frequency responses of the axial and radial displacements consider all the circumferential modes in the range $n=0:10$. With a greater contribution of axial excitation, the axial response is mainly dominated by axial resonances. Similarly, with a greater contribution of radial excitation, the radial response is mainly dominated by the bending modes. Furthermore, increasing the weighting of the axial force increases the amplitudes of the axial response, and similarly, increasing the weighting of the radial force increases the amplitudes of the bending modes for the majority of the frequency range.

CONCLUSIONS

A low frequency model of simplified physical model of a submarine hull has been presented. The submerged hull was modelled as a fluid-loaded cylindrical shell closed at each end by circular plates. Two cases of excitation were considered, corresponding to axial excitation at the centre of one end plate and radial excitation at the edge of the end plate. For the axisymmetric case corresponding to axial excitation at the centre of the end plate, the zeroth ($n=0$) circumferential shell modes are predominantly excited. Similarly, under radial excitation at the edge of the end plate, the bending ($n=1$) circumferential hull modes are predominantly excited. Under simultaneous axial and radial excitation, the axial displacement is mainly dominated by the axial excitation while the radial response is mainly dominated by radial excitation.

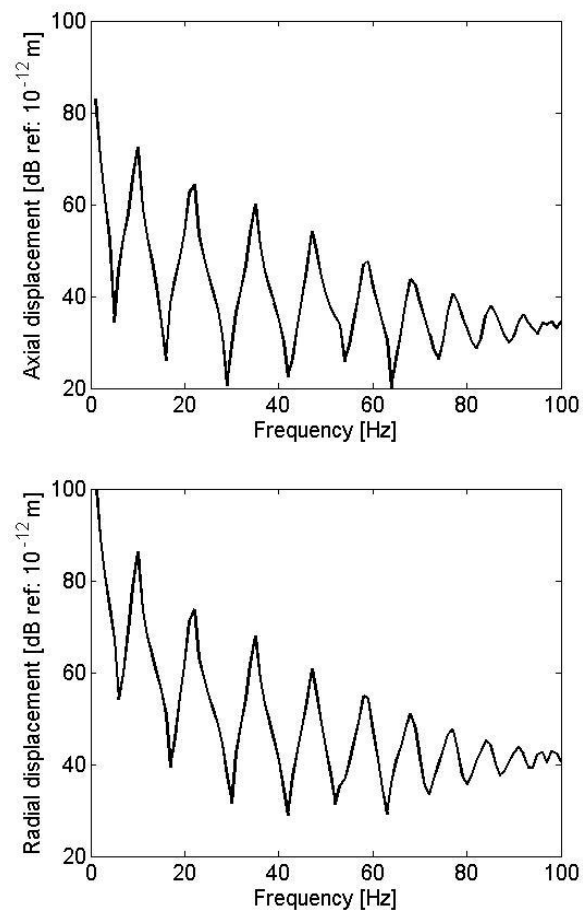


Figure 6. Axial and radial responses due to radial excitation at the edge of the end plate ($\alpha=0$ and $\beta=1$)

REFERENCES

Amabili, M and Paidoussis, MP 2003, *Review of studies on geometrically nonlinear vibrations and dynamics of circular cylindrical shells and panels, with and without fluid structure interaction*, Applied Mechanics Reviews, vol. 56, no. 4, pp. 349-381.

Breslin, JP and Andersen, P 1994, *Hydrodynamics of ship propellers*, Cambridge University Press.

Caresta, M and Kessissoglou, NJ 2010, *Acoustic signature of a submarine hull under harmonic excitation*, Applied Acoustics, vol. 71 pp. 17-31.

Caresta, M and Kessissoglou, NJ 2011, *Reduction of hull-radiated noise using vibroacoustic optimization of the propulsion system*, Journal of Ship Research, vol. 55, no. 3, pp. 149-162.

Forsberg, K 1964, *Influence of boundary conditions on the modal characteristics of thin cylindrical shells*, AIAA Journal, vol. 2, pp. 2150-2157.

Galletly, GD and Mistry, J 1974, *The free vibrations of cylindrical shells with various end closures*, Nuclear Engineering and Design, vol. 30, no. 2, pp. 249-268.

Junger, MC and Feit, D 1986, *Sound, structures, and their interaction*, Cambridge, MIT Press.

Leissa, AW 1993, *Vibration of shells*, American Institute of Physics, Woodbury, New York

Mukhopadhyay, M and Sinha, G 1992, *A review of dynamic behaviour of stiffened shells*, Shock and Vibration Digest, vol. 24, no. 8, pp. 3-13.

Scott, JFM 1988, *The free modes of propagation of an infinite fluid-loaded thin cylindrical shell*, Journal of Sound and Vibration, vol. 125, pp. 241-80.

Tso, YK and Hansen, CH 1995, *Wave propagation through cylinder/plate junctions*, Journal of Sound and Vibration, vol. 186, no. 3, pp. 447-461.

Yu, YY 1955, *Free vibrations of thin cylindrical shells having finite lengths with freely supported and clamped edges*, Journal of Applied Mechanics, vol. 22, pp. 547-552.

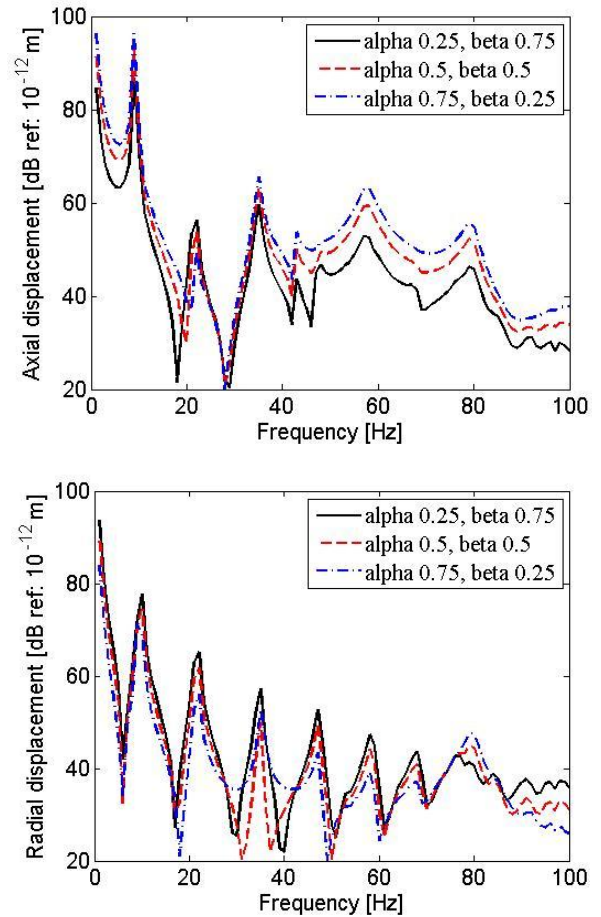


Figure 7. Comparison of simultaneous axial and radial excitation for different weightings